Journal of Rehabilitation in Civil Engineering 9-1 (2021) 52-70

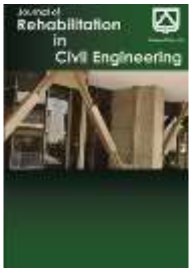

journal homepage: http://civiljournal.semnan.ac.ir/

An Experimental Study on Effect of Concrete Type on Bond Strength of GFRP Bars

A. DoostMohamadi[1*], A. Vatani Oskouei[2] and A. Kheyroddin[3]

1. M.Sc. Graduated, Department of Civil Engineering, Shahid Rajaee Teacher Training University, Tehran, Iran
2. Associate Professor, Department of Civil Engineering, Shahid Rajaee Teacher Training University, Tehran, Iran
3. Professor, Faculty of Civil Engineering, Semnan University, Semnan, Iran

Corresponding author: *alireza.dm71@gmail.com*

ARTICLE INFO

Article history:
Received: 28 February 2020
Accepted: 23 May 2020

Keywords:
Reinforced concrete,
Bonding resistance,
GFRP bar,
Macro-synthetic fiber,
Light-weight concrete.

ABSTRACT

One of the common methods to create bond strength in reinforced concrete is providing development length. The bond strength of glass fiber reinforced polymer (GFRP) bar is inherently poor due to its shape, as well as its inadequate mechanical interlocking with concrete. Therefore, providing sufficient development length in this bar is different and more conservative in comparison with steel bars. In this study, three types of concrete are selected, namely normal-weight concrete (NWC), light-weight concrete (LWC), and light-weight fiber reinforced concrete (LFRC). In order to investigate the adequate development length required for GFRP bars and its relation with the concrete type and compressive strength, for Each type of concrete, two different mix designs which have various compressive strengths are considered. 18 cube specimens are fabricated and the direct pull-out test is performed. The results indicate that, in all types of concrete, as the compressive strength increases, the bond strength between concrete and rebar augments. In addition, assessing the bond strength of different types of concrete demonstrates that the use of LWC, due to its inherent weakness of aggregates interlocking, causes pre-mature cracks and loss of the bond strength compared to NWC. Furthermore, LFRC mixtures containing 0.3% and 0.5% macro-synthetic fiber volume fraction reveal that the presence of fibers can be effective in controlling cracks and increases the bond strength between GFRP bars and concrete. As a result, with the increase of the bond strength between the GFRP bar and the concrete, the ultimate capacity of the concrete cross-section augments.

DOI: 10.22075/JRCE.2020.19922.1392

1. Introduction

Using traditional steel bars is a common method to reinforce concrete. Nowadays, utilizing fiber-reinforced polymer (FRP) bars has increased as a new generation of bars for the reinforcement. Many advantages such as high tensile strength, corrosion resistance, light weight, and resistance to thaw and frost [1–4] have made them as a decent alternative to traditional steel bars in the harsh environmental conditions. Moreover, a tendency to use of FRP bar in geotechnical engineering practices as a promising solution to eliminate the corrosion problem have been considered as an alternative for common steel reinforcement [5]. However, some drawbacks such as lack of ductility behavior, low modulus of elasticity, and lower bond strength compared to steel bars are the weaknesses of FRP bars [6]. Also, using FRP bar may cause a brittle failure in reinforced concrete (RC) while FRP sheets can used for increasing ductility [7,8].

As using FRP bars to reinforce concrete has increased, understanding the performance of utilizing these two materials together is crucially significant; it also helpful to comprehend the behavior of FRP bar reinforced concrete, as well as estimate the members' structural capacity. In this regard, one of the effective parameters is the bonding strength between concrete and FRP bar. Indeed, the bonding is the reason for the composite behavior of reinforced concrete which transfers the force between the concrete and the bar owing to the friction. Some of the main factors affecting the bond strength between concrete and FRP bar, are bar diameter, embedment length, concrete compressive strength, bar confinement conditions, and bar appearance in terms of ribs shape [9]. It is worth mentioning that the cast direction also influences the bond strength. In a research study by Golafshani [10], the effect of horizontal and vertical cast directions of longitudinal GFRP bar on the bond strength was assessed. The results indicated that the specimens with the horizontal casting had slightly higher bond strengths in comparison with the vertical casting.

So far, many research studies have been done on the influence of the aforementioned parameters. For instance, in the similar studies conducted by Benmokrane et al. [11] and Al-Zahrani [12], the relationship between the embedment length and the bond strength was investigated. The results of these studies showed that a double increase of the FRP bar embedment length from 63.5 mm to 127 mm with a constant diameter of 12.7 mm, led to 15 to 25% reduction in the bond strength in all the specimens. Furthermore, in other research conducted by Saleh et al. [6], increasing the embedment length from 5 times the bar diameter to 10 times the bar diameter caused relatively lower bond strength in high-strength concrete. Actually, the longer embedment length can make an increase in the maximum tensile force; on the other hand, enhancing the embedment length leads to a larger contact surface between the bar and concrete. consequently, due to the non-linear distribution of the bond stresses, lower bond stress was obtained [13]. Hence, only the increase of the FRP bar embedment length cannot be an efficient solution to enhance the bond strength between concrete and FRP bars.

Regarding the impact of bar diameter, many studies have been conducted [9,14–17]. Al-Zahrani et al. [18] considered the diameter of the FRP bar as a variable with the values of

12.7, 15.9, 19.1, and 25.4 mm. In this study, the embedment length was constant and equal to 127 mm. The results demonstrated that as the bar diameter increased, the bond strength decreased [18–20]. One of the reasons could be the variability of the shear stress distribution around the polymer bar. Also, the decline in the bond strength due to the increase of the bar diameter could be attributed to the shear lag and Poisson effect [21]. All in all, it is concluded that using high diameter FRP bars may come across difficulties in order to provide the adequate bond strength which affects the development length as well.

There are other studies which investigate the effect of the compressive strength on the bond strength. In the research conducted by Ashrafi et al. [22], compressive strength was one of the variables whose values were considered 16, 24, and 37 MPa for normal-weight concrete. The values of the bond strength obtained in this study were 9.33, 9.58 and 10.41, respectively. Therefore, the increase of the compressive strength results in the enhancement of the bond strength as confirmed by other studies [10,23].

The effect of concrete type is one of the parameters that recently have become appealing to researchers. Zemor et al. [14] studied the bond strength of the FRP bar in normal-weight concrete and normal-weight self-compacted concrete. The bond strength was measured in the bending test and the results showed that the use of self-compacting concrete could increase the bond strength. The bond strength of both steel and GFRP bars in self-compacting concrete were relatively higher than that of the normal weight concrete; this can be due to the uniform mixture of the concrete matrix [10,24]. Moreover, The mixes made of poly-carboxylate-based super plasticizer had the most compressive and tensile strengths compared to other super plasticizer types [25] which directly influenced the bond strength. Light-weight concrete as a new generation of concrete material offers many advantages such as lower effective weight of structures, which allows to have larger spans and causes reduction in structural members' dimensions owing to the less applied dead-load [26]. A research study carried out by Doostmohamadi A. et all [23] revealed that the failure mode of the bond behavior between GFRP bar and light-weight concrete was brittle in both light-weight concrete and GFRP bar rupture; At issue is that lower effective weight as light-weight concrete could be, ultimate failure in a brittle manner may cause an unfavorable failure; as a solution, the use of fiber reinforced concrete was suggested by the authors. Also, it has been proved by other researchers that splitting failure never occur due to the presence of fiber [23,27]. Indeed, fibers' bridging mechanisms prevent the degeneration of micro-cracks into macro-cracks [16]. Using concrete with fibers has improved the bonding behaviour of concrete mixture and its application specially in connecting prefabricated elements has been widespread recently [28]. Considering the effectiveness of fiber reinforced concrete, a research program was performed by Varona et al. [27] to assess the impact of steel fibers on the bond strength of steel bars reinforced concrete. In this study, the fiber consumption in the mix design was 20 kg per cubic meter. Moreover, two different types of steel fibers with diameters of 0.75 and 0.35 mm, lengths of 35 and 30 mm, dimension ratios of 46.7 and 85.7, and tensile strengths of 1200 and 3000 MPa were used, respectively. The results showed that using fibers with the higher aspect ratio and higher tensile strength increased the bond strength by 90%. Also, another study by FakhriFar et al. [29] indicated that the use of polypropylene fibers in the range of 0.5 to 1% volume fraction could significantly improve the mechanical properties of the concrete and its ability to control cracking as well. In fact, using macro-synthetic fibers could ameliorate the both mechanical and durability properties of the concrete [30]. This could be because fiber bridging in the entire matrix of concrete could effectively control cracking; as a result, the shear cracks around the bar could be restrained in terms of width and propagation during the pull-out [23]. The bond behavior between GFRP bars and hybrid fiber reinforced concrete (HFRC) can be improved by the cooperative effects of different types of fibers such as Carbon, Aramid, and Polypropylene. increasing the volume fraction of fiber leads to an improvement of the bond behavior and ductility performance between the GFRP bars and the HFRC [19].

It is worth mentioning that there are different methods to evaluate the bond strength between bar and concrete. Direct pull-out [6,10,15,20,22,23,31–33] and beam tests [17,34,35] have been the most common ones in this regard. Despite the fact that the bending test simulates the bond conditions of a reinforced concrete member almost well; in many studies, the direct pull-out test has been chosen to investigate the bond behavior because of its simplicity. It should be mentioned that the results of pull-out test are affected by the confinement applied to the surrounding concrete during the test process [36]. A comparative study about the differences between direct pull-out and beam tests was conducted by F. De Almeida Filho et al. [37]. The results of the aforementioned study demonstrated that the specimens with the compressive strength value of 30 MPa, attained similar bond strengths in the both methods, pull-out and beam tests. On the other hand, in those specimens with the higher compressive strength value, 60 MPa, results were quite different in terms of slippage, more slippage recorded in the pull-out test; however, the bond strengths were almost similar. Moreover, O. Gooranorimi [38] established a relationship for the bond-slip model [39] which was obtained by direct pull-out test in order to evaluate the flexural behavior of GFRP reinforced concrete slabs considering the effect of bond slippage.

In the present study, due to the extended use of concrete technology and new materials such as GFRP bars and light-weight concrete, it is attempted to investigate the behavior and bond strength of GFRP bar in normal weight, light-weight, and light-weight fiber reinforced concrete. To do so, in the first step, a study is carried out on the effect of compressive strength on the bond strength of GFRP bar with both normal-weight concrete and light-weight concrete. In the second step, considering the concrete specimens with the same compressive strength values, a comparison between normal-weight and light-weight concrete is done and the impact of concrete type is assessed. Finally, in the last step, macro-synthetic fibers with two different volume fraction values are utilized to improve the shear strength of light-weight concrete and its bond strength with GFRP bar.

2. Experimental Program

To investigate the bond strength of GFRP bars in different types of concrete, three various types of concrete are considered, namely normal-weight concrete (NWC), light-weight concrete (LWC), and light-weight fiber reinforced concrete (LFRC). Then, 18 specimens are fabricated and cured for 28 days. Finally, direct pull-out test has been carried out on the 60-day-old specimens.

2.1. Specimen Description

In the present study, 18 specimens which include six different concrete mix designs are tested. All the specimens are fabricated using sand coated glass fiber reinforced polymer (GFRP) bars with a nominal diameter of 8 mm. The concrete mix designs of normal-weight concrete specimens are denoted as NWC1 and NWC2 with 27 and 38 MPa compressive strengths, respectively; The concrete mix designs of light-weight concrete specimens are named LWC1 and LWC2 with the compressive strength of 26 and 37 MPa, respectively; and The concrete mix designs of lightweight fiber-reinforced concrete specimens are denominate LFRC1 and LFRC2 with the compressive strength of 38 and 36 MPa, respectively. The specimens are fabricated in cubes with the size of 15×15×15 cm, and the GFRP bar is placed in the center of the concrete as shown in Fig. 1. The mold of all the specimen are drilled in such a way that the free end of the bar can pass through the mold, since it is needed to measure the bar slippage during the test. In addition, Fig. 2 shows the placement of GFRP bar in the concrete. The embedment length of rebar is assumed 10 times GFRP bar's diameter in all the specimens. The both ends of GFRP bars at the edge of the concrete are considered without any contiguity with the concrete surface in order to provide the desired embedment length. Table 1 presents the characteristics of the specimens in detail.

Table 1. Specimens characteristics details.

Specimen code	Concrete type	Compressive strength (MPa)	GFRP-bar diameter (mm)	Bar embedment length (mm)
NWC1	Normal-weight concrete	27	8	80
NWC2	Normal-weight concrete	38	8	80
LWC1	Light-weight concrete	26	8	80
LWC2	Light-weight concrete	37	8	80
LFRC1	Light-weight fiber reinforced concrete	38	8	80
LFRC2	Light-weight fiber reinforced concrete	36	8	80

Fig. 1. a) Casting molds b) Prepared samples for direct pull-out test.

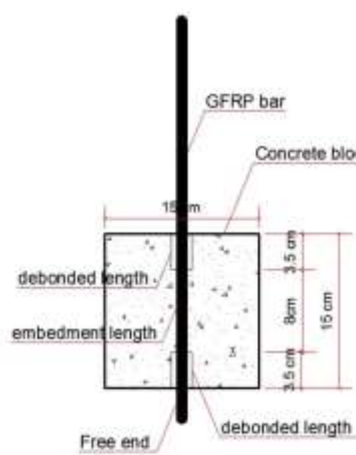

Fig. 2. The placement of GFRP bar embedded in concrete.

2.2. Material Properties

2.2.1. Concrete

In this paper, six concrete mix designs with three types of concrete namely, Normal-weight concrete, light-weight concrete, and light-weight fiber reinforced concrete, with different compressive strengths are used. The cement type utilized in the present study is Type 2 that is manufactured by Tehran Cement Plant and its chemical specifications is presented in Table 2. For all three types of concrete, fine aggregate is river sand type with the soft modulus of three. Coarse aggregate used in normal-weight concrete is natural gravel; but in both light-weight and light-weight fiber reinforced concrete, light expanded clay aggregate (Leca) with the specific gravity of 580 ($\frac{kg}{m^3}$) is utilized as coarse aggregate. The physical and mechanical properties of each mix design are detailed in Table 3. The purpose of selecting the mix designs presented in Table 3 is to study the bond strength of rebar and concrete, considering different types and compressive strengths. To do so, in the first phase, a comparative study is done on the effect of increasing compressive strength in the both normal-weight concrete (NWC) and light-weight concrete (LWC) specimens. Then, in the second phase, considering almost equal compressive strength values of LWC1 and NWC1, as well as LWC2 and NWC2, the effects of using normal-weight concrete and light-weight concrete on the bond strength are determined. Due to the fact that the inter-locking of light-weight concrete is generally weaker than that of the normal one which leads to pre-mature cracking of the light-weight concrete. This can cause the loss of bond strength between bar and concrete relatively in lower bond strength than NWC's specimens. In the last phase, in order to compensate the inherent weakness of Light-weight concrete, Macro-synthetic fibers are used. Light-weight fiber reinforced concrete mix designs with two different fiber volume fractions of 0.3% and 0.5% are selected in LFRC1 and LFRC2, respectively, in confirmation with ASTM C1116 [40] to evaluate the impact of fiber content on the bond strength as well.

Table 2. Chemical properties of cement.

Material	Chemical analysis (%)									Specific surface (cm^2/gr)
	SiO_2	Al_2O_3	Fe_2O_3	CaO	MgO	SO_3	Na_2O	K_2O	L.O. I	
Cement	91.7	1.2	1.1	1.7	0.9	0.2	0.5	0.7	2	200000

Table 3. Mechanical and physical properties of concrete.

Mix design code	NWC1	NWC2	LWC1	LWC2	LFRC1	LFRC2
$compressive\ strength\ (MPa)$	27	38	26	37	38	36
$modulus\ of\ elasticity\ (MPa)$	26280	31225	18820	23720	26550	27610
$density\ (kg/m^3)$	2286	2314	1892	1920	1930	1926
$fiber\ volume$ (%)	0	0	0	0	0.3	0.5
$fiber\ content\ (kg/m^3)$	0	0	0	0	2.7	4.5
$fine\ aggregate\ (kg/m^3)$	Sand (1000)	Sand (1000)	Sand (1000)	Sand (1000)	Sand (1000)	Sand (1000)
$coarse\ aggregate\ (kg/m^3)$	Gravel (650)	Gravel (650)	Leca[1] (220)	Leca[1] (220)	Leca[1] (220)	Leca[1] (220)
$lime\ stone\ powder\ (kg/m^3)$	225	225	225	225	225	225
$cement\ (kg/m^3)$	350	390	350	390	390	390
w/c	0.5	0.4	0.5	0.4	0.4	0.4
$slump\ (mm)$	105	90	110	95	85	75

[1]Lightweight expanded clay aggregate

2.2.2. GFRP bar

In this study, all the specimens are made using sand coated GFRP bar with a nominal diameter of 8 mm, as shown in Fig. 3. In order to assess mechanical properties of GFRP bar, a tensile strength test is done according to ASTM-D7205 [41]. The mechanical and physical properties of GFRP bar, including modulus of elasticity, maximum tensile strength, rupture strain, and specific weight are presented in Table 4. Furthermore, the stress-strain diagram of GFRP bar is plotted in Fig. 4.

Fig. 3. Sand-coated GFRP bar.

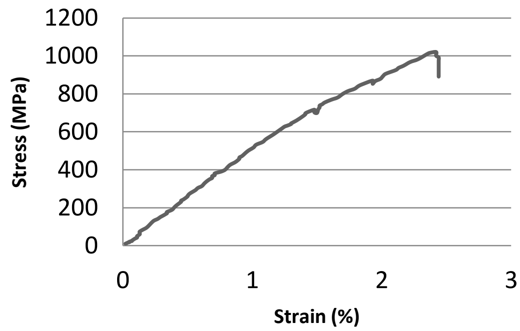

Fig. 4. Stress-strain curve of GFRP bar.

Table 4. Physical and mechanical properties of GFRP bar.

Bar type	Diameter (mm)	Tensile strength (MPa)	Modulus of elasticity (GPa)	Strain (%)	Density (gr/cm^3)
Sand coated GFRP	8	1024	50	2.3	2.2

2.2.3. Fiber

As shown in Fig. 5, Emboss macro-synthetic fiber manufactured by Sirjan-nano Company is used in the light-weight fiber reinforced concrete (LFRC) mix designs. Based ASTM D7508 [42] the fiber chemical structure is polyolefin-based. Physical and mechanical properties of the fiber are guaranteed by the producer according to ASTM D2256 [43] as presented in Table 5.

Table 5. Physical and mechanical properties of Emboss macro-synthetic fiber.

Diameter (mm)	Length (mm)	Aspect ratio (L/D)	Tensile strength (MPa)	Modulus of elasticity (GPa)	Strain (%)	Density (gr/cm^3)
0.4	40	100	600	6.4	10	0.91

Fig. 5. Emboss macro-synthetic fiber used in LFRC1 and LFRC2.

2.3. Set up and Instrumentation

In order to investigate the bond strength of GFRP bar and concrete, the direct pull-out test is carried out using universal testing machine (UTM) according to ASTM-D7913 [32]. As shown in Fig. 6, a steel frame is employed as a configuration tool to restrain the concrete movement and a tensile force is applied to the GFRP bar based on the proposed testing method by Bazli et al. [22].

The specimen is placed in the middle of the steel frame and one side of the bar is inserted into the grip and the other free end is attached to a linear variable displacement transducer (LVDT-1). Another (LVDT-2) is installed on the top of the steel frame to measure its axial deformation. Finally, the actual slip rate of the GFRP bar in the concrete is obtained from the difference between the displacements measured by LVDT-2 and LVDT-1. The test is run in a displacement controlled mode with a constant loading rate of 1.2 mm/min. The test is continued to reach one of the following failure cases based on Canadian Standards Association [44] (a) tensile failure in GFRP bar, (b) concrete failure by splitting, or (c) bond failure with the slippage of more than 5 mm with a constant force. Fig. 6 shows the test set up with the steel frame, LVDTs, and universal testing machine.

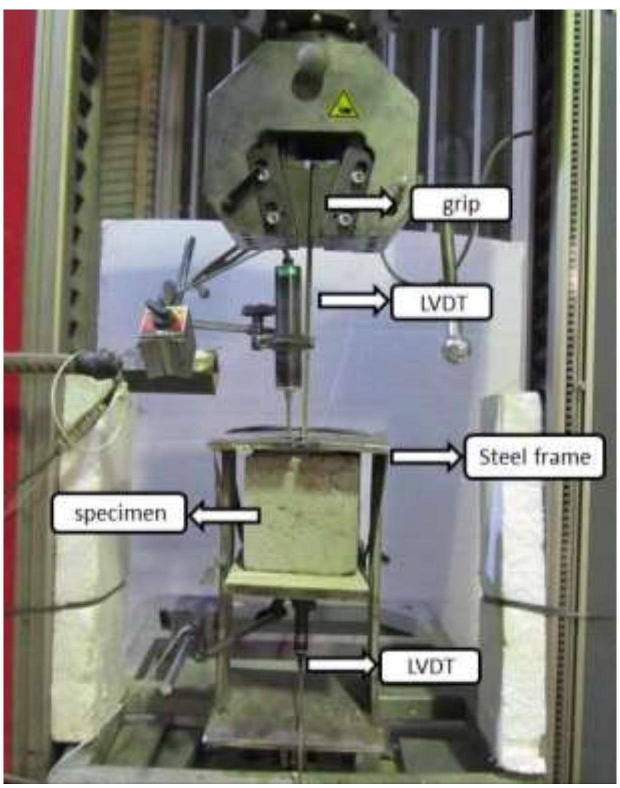

Fig. 6. Test setup and configuration.

3. Results and Discussion

The measured parameters obtained from the direct pull-out test in this research are as follows: failure type of each specimen, ultimate bond stress (τ) obtained from Equation 1, maximum tensile force in the GFRP bar (P_{max}), maximum tensile stress in the GFRP bar (f_f), the ratio of the tensile stress to the maximum tensile strength of GFRP bar $(stress\,ratio)$ obtained from Equation 2 and 3. In the aforementioned equations, parameters D, A_{bar}, and l are GFRP bar diameter, GFRP bar cross section area, and embedded length, respectively. It is worth mentioning that the ultimate bond stress (τ) is considered as a main comparative parameter for the enhancement of stress level affected by different types of concrete and compressive strength. In order to scrutinize the results, each test is repeated three times. The summary of the test results are presented in Table 6.

$$\tau = \frac{P_{max}}{\pi D l} \quad (1)$$

$$f_f = \frac{P_{max}}{A_{bar}} \quad (2)$$

$$stress\,ratio = \frac{f_f}{f_{fu}} \quad (3)$$

3.1. Load-Free End Slip Curve

In this section, the results of the load-free end slip curve and the failure mode for all the specimens are discussed. Stress-free end slip diagrams for specimens NWC1, NWC2, LWC1, LWC2, LFRC1, and LFRC2 are plotted in Fig. 7 so as to investigate the influence of the concrete type and its compressive strength on the bond strength between concrete and GFRP bar. The stress-free end slip diagram in Fig. 7 shows that at the beginning of the test, due to the chemical adhesion strength between the GFRP bar surface and the cement matrix, the curve is completely vertical with infinite slope while the GFRP bar has no slippage in the concrete it should be noted that this is also proved by other studies [22,23]. With the deterioration of the chemical adhesion, the mechanical bonding strength is created as the GFRP bar surface becomes involved with the concrete. According to the results, it can be claimed that the primary adhesion strength depends on the compressive strength of the concrete, and for the higher compressive strength of the concrete, the slope of the graph starts at a higher point, as proved in other research [22,23].

Table 6. Summary of the test results.

Specimen code	Peak load (kN)	Bar maximum tensile stress (MPa)	Stress ratio (%)	Bond strength (MPa)	Failure mode
NWC1	15.55 (1.27)*	309.51 (29.18)	30 (3)	7.74 (0.73)	bond Failure (concrete crushing)
NWC2	19.54 (1.57)	388.93 (31.27)	38 (3)	9.72 (0.78)	bond Failure (concrete crushing)
LWC1	11.82 (1.27)	235.27 (25.37)	23 (2)	5.88 (0.63)	bond Failure (concrete crushing)
LWC2	13.05 (1.31)	259.75 (26.06)	25 (3)	6.49 (0.65)	bond Failure (concrete crushing)
LFRC1	17.04 (1.6)	339.17 (31.86)	33 (3)	8.48 (0.79)	bond Failure (concrete crushing)
LFRC2	19.54 (1.57)	383.96 (37.61)	37 (4)	9.6 (0.94)	bond Failure (concrete crushing)

*The numbers in parenthesis denote the standard deviations

It should be noted that the failure mode while the bond strength exists between the concrete and the GFRP bar, can comprise three modes as follows: 1) bond failure: in this case, ribs are detached from the bar. It is worth mentioning that the weakness of the bond strength between the ribs and the bar cannot be compensated by increasing the concrete compressive strength or changing its type. Also in this case, there is another type of failure due to the cracking inside the concrete which can reduce the bond stiffness and cause the slippage of the bar in concrete; thus, the increase of the compressive strength and the type of concrete can affect the bond strength. 2) Bar Rupture: in this mode, the concrete bond strength is enough to reach the ultimate tensile capacity of the bar; and the rupture occurs at the cross section of the bar under the tension which is a brittle failure. 3) Concrete splitting: in this case, because of the weak compressive strength of the concrete and consequently lower shear strength, cracks appear on the concrete surface and the bond strength between the concrete and the bar vanishes before the bar reaches its maximum tensile strength.

In this study, all the specimens are failed according to the first mode and with the appearance of cracks inside the concrete which cause the decline of the bond stiffness and slippage of the bar in the concrete. In these experiments, 5 mm slippage of the bar is utilized as an acceptance criterion for the bond strength loss [44]. This limitation is shown in the load-free end slip curve in Fig. 7 as a dashed line. However, in the present study, the test is continued for the higher values of the bar slippage inside the concrete which is shown in Fig. 6.

The diagram in Fig. 8 shows the maximum bond strength of the specimens. In the specimens made of normal-weight concrete, the bond strengths of 7.74 and 9.72 MPa are obtained for specimens with the compressive strength of 27 and 38 MPa, respectively. These results show that the increase of compressive strength in normal-weight concrete causes 25% enhancement in the bond strength. In the light-weight concrete specimens, the bond strength of 5.88 and 6.49 MPa is gained for the specimens with 26 and 37 MPa compressive strength, respectively. Therefore, similar to normal-weight concrete, enhancing the compressive strength, leads to the increase of the bond strength in light-weight concrete as well; but the increase in LWC is about 11% which is relatively less than the enhancement in the NWC. Because inter-locking of light-weight aggregate is less than that of the normal one, the increase of the compressive strength has less effect on the enhancement of the bond strength in light-weight concrete. In this study, macro-synthetic fibers are used to compensate for this weakness. The results of both light-weight fiber reinforced concrete specimens which relatively have the same compressive strength values (36 and 38 MPa) but different fiber volume fractions, show the bond strengths of 8.48 and 9.6 MPa for LFRC1 and LFRC2, respectively. The bond strength values of LFRCs are relatively close to that of NWC2. This demonstrates that fibers can play a vital role in delaying the creation of the pre-mature crack in light-weight concrete. The reason behind the fact is the random dispersion of fibers in the concrete matrix, since many of fiber filaments are in convergence with shear cracks [45]; so, they can limit the crack width and avoid the bond loss. It should be noted that increasing the fiber volume fraction from 0.3 percent to 0.5 percent, can enhance the bond strength by 13%.

Fig. 9 and Fig. 10 display the maximum stress created at the GFRP bar cross-section and the ratio of the maximum tensile stress developed in the GFRP bar cross-section to its ultimate tensile strength. In fact, Fig. 10 shows the maximum available capacity of the GFRP bar before the bond loss. The maximum reachable tensile capacity of GFRP bars are 0.38, 0.37, 0.33, 0.30, 0.25, and 0.23 for NWC2, LFRC2, LFRC1, NWC1, LWC2, and LWC1 specimens, respectively. A comparison among these values indicates that the use of macro-synthetic fibers can significantly increase the reachable tensile capacity of GFRP bars in light-weight concrete.

In general, it can be concluded that the use of GFRP bars without a proper restraint causes pre-mature bond loss; furthermore, the reachable tensile capacity in GFRP bar cross section of the concrete members is less than 50% of their ultimate tensile strength. This may lead to a significant reduction in the ultimate flexural and shear capacity, and a higher crack width in the concrete members. Therefore, using a proper concrete type according to the design criteria and the required stress level at the GFRP bar cross-section is essential. It is worth to mention that the designated tensile stress levels in GFRP bar cross-section, accordingly the required bond strength need to be addressed in the design process.

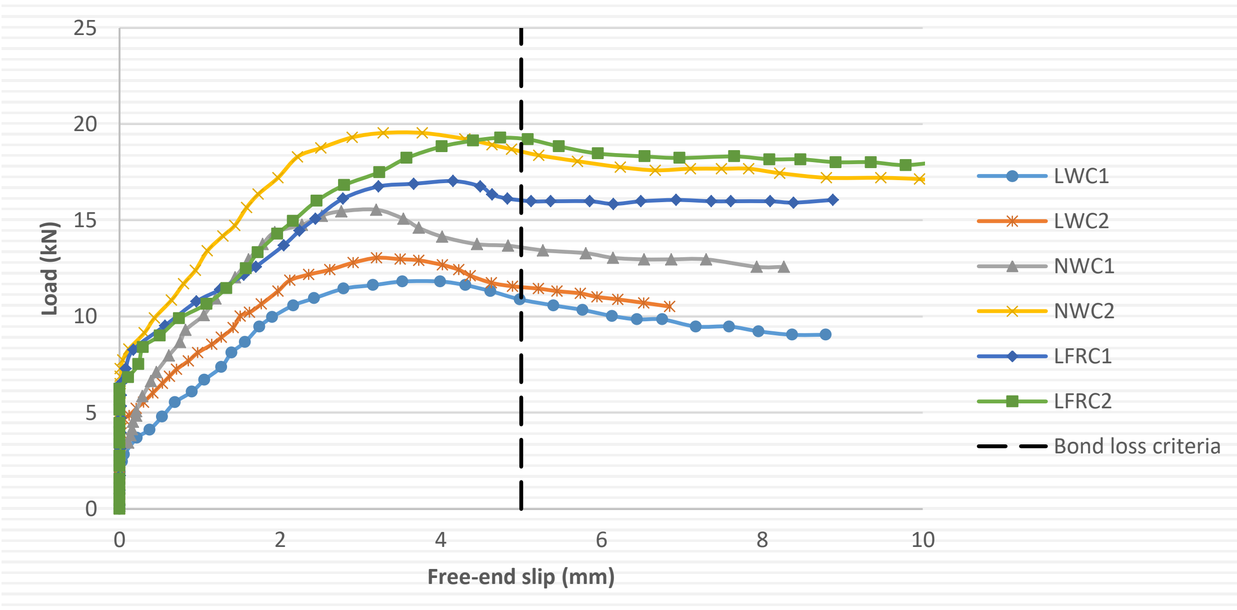

Fig. 7. Load-free end slip curve.

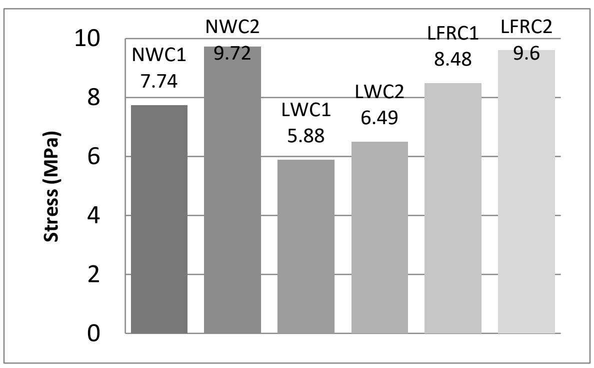

Fig. 8. Maximum bond strength in specimens.

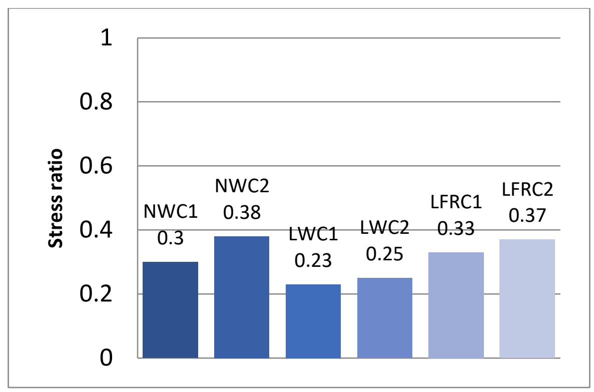

Fig. 10. Maximum tensile stress ratio developed in GFRP bar cross-section.

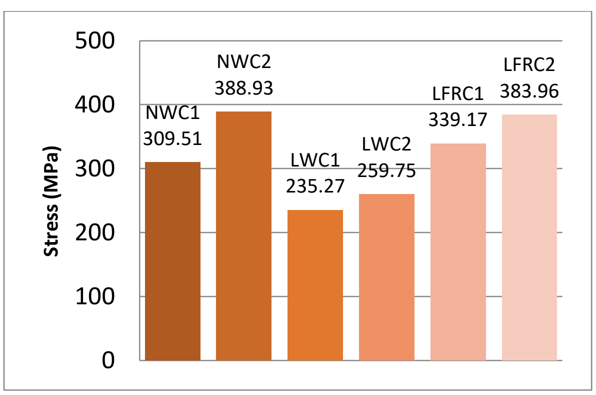

Fig. 9. Maximum tensile stress developed in GFRP bar cross section.

3.2. Failure Mode

At the end of the tests, no signs of extensive concrete damages or bar ruptures are observed in the specimens. Fig. 11 and Fig. 12 show NWC1 and NWC2 specimens, respectively, at the end of the test. The bar slippage at the free end and the absence of extensive cracks on the surface of specimens indicate that the bond loss failure mode is occurred. Due to the inside cracking of the concrete, bar slippage eventually reaches to the amount of higher than 5 mm. Fig. 13 and Fig. 14 display LWC1 and LWC2 specimens' failure, respectively. In the both specimens, bar slippage at the free end side is obvious. As shown in Fig. 14a, LWC2 is slightly cracked up to the surface. As it is obvious in Fig. 14c, the cracks created around the bar in the concrete are grown to the surface, which is due to the continuation of the test until the slippage is higher than 5 mm. Increasing the compressive strength of concrete causes cracks to develop at the higher amounts of the bond strength. As a result, the tensile stress increases in the GFRP bar cross-section. Also, Fig. 15 and Fig. 16 show LFRC1 and LFRC2 specimens' failure mode, respectively. In fact, the presence of fibers in these specimens creates cracks with smaller widths in comparison with LWC2. Furthermore, the tensile stress level in the GFRP bar cross-section achieves the higher amount than that of the light-concrete because the fibers can bridge the inner cracks to avoid propagating the cracks inside of the concrete; consequently, the bond strength increases.

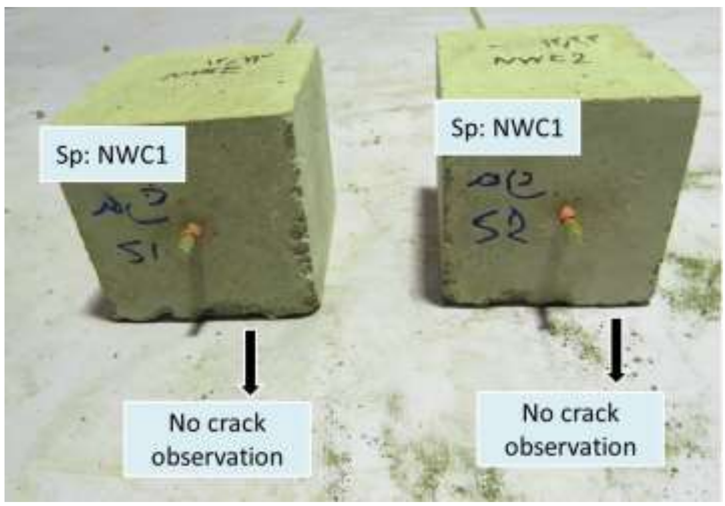

Fig. 11. Bar slippage occurred in specimen NWC1.

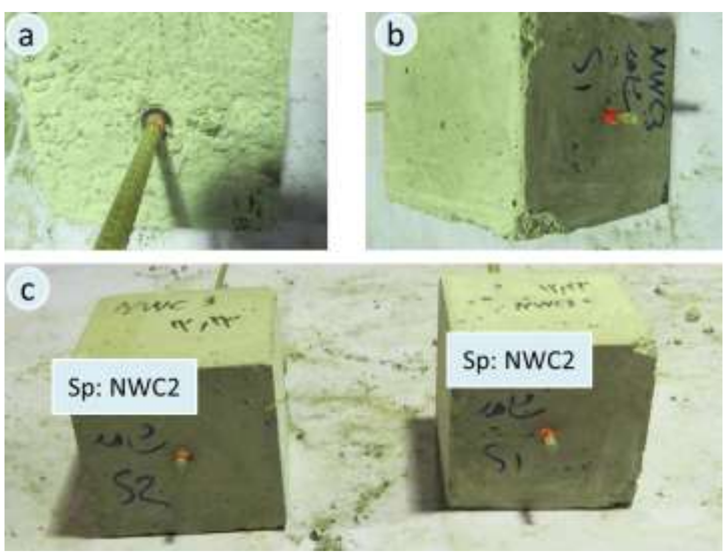

Fig. 12. a) No crack observation on the top surface b) No crack observation on the side surfaces c) Free end slippage occurs.

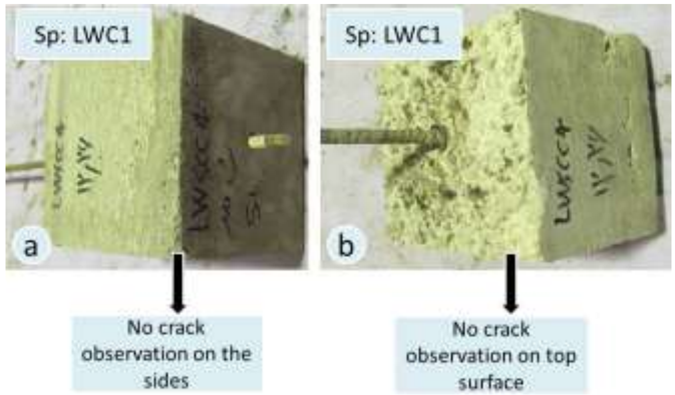

Fig. 13. a) No crack observation on the side surfaces b) No extended crack observation on the top surface during the bar slippage.

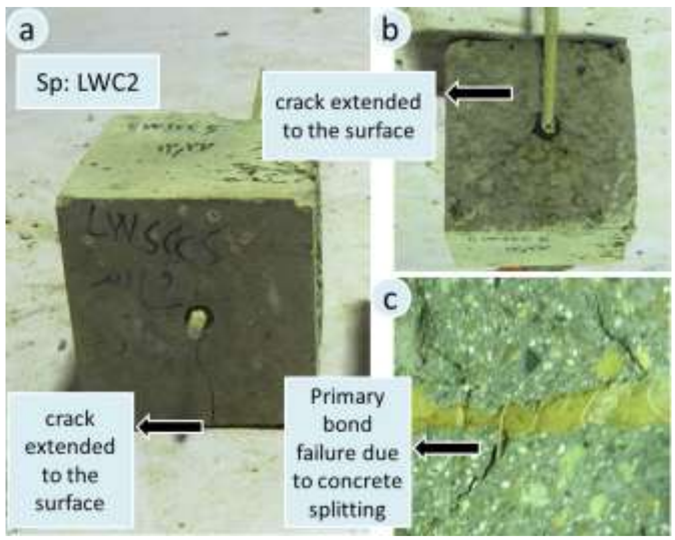

Fig. 14. a) Extended crack on the bottom surface b) extended crack on the top surface c) primary cracks due to the bar slippage and lack of enough shear strength.

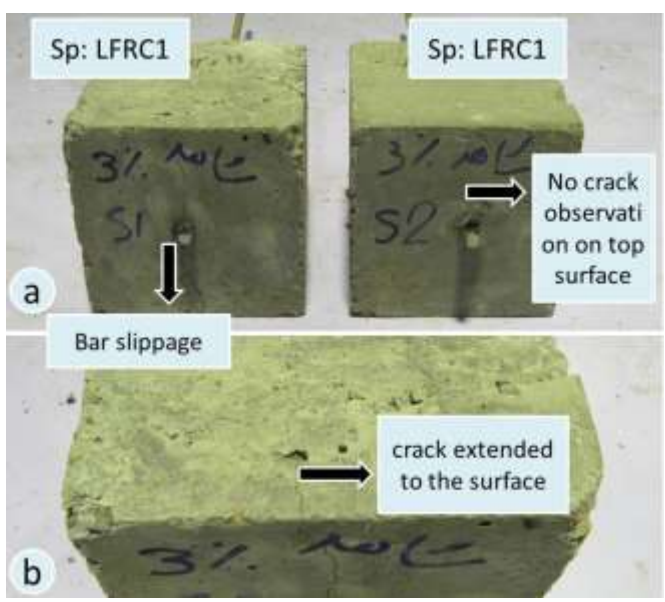

Fig. 15. Bar slippage occurred for specimen LFRC1.

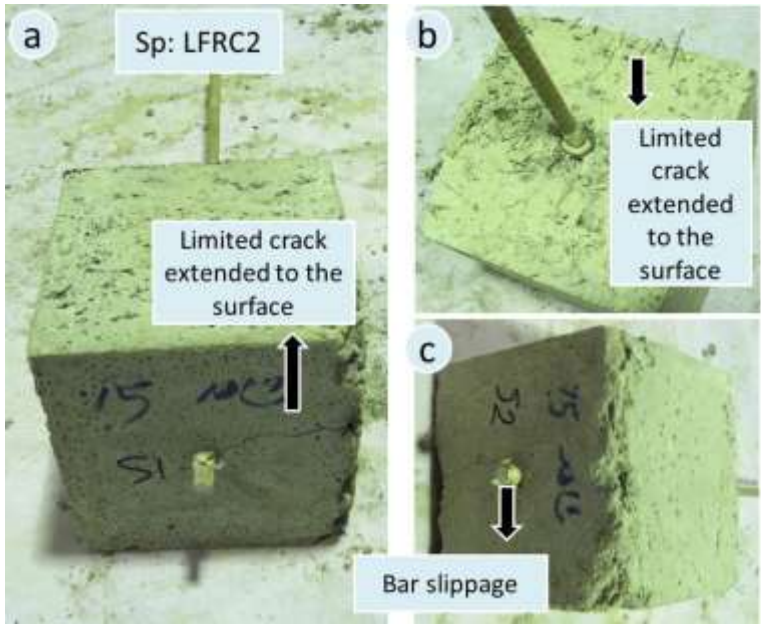

Fig. 16. Bar slippage occurs for specimen LFRC2.

3.3. Design Codes

To ensure adequate bonding resistance between bar and concrete, the existing Design guidelines for concrete structures suggest methods which provide development lengths, use hooks or utilize mechanical restraints. In each of the proposed solutions, formulas are provided by the codes. In order to comprehend the results of this research, the formula in section 3.3.1 and 3.3.2 of the design codes are presented to compare the required development length, needed for calculating the bar stress, to the experimental results from each specimen. Generally, the tensile force created in the bar is transmitted through the bond between the concrete and the bar. Fig. 17 shows the mechanism of this transfer and Equation 4 is obtained using the balance between the forces. In Equation 4, the parameters l_e, d_b, u, A_f, and f_f are development length, bar diameter, the bonding strength between bar and concrete, bar cross-section area, and bar cross-section tensile stress, respectively. By testing the specimens, the parameter indicating the bond stress between concrete and GFRP bars are obtained for all the specimens. Using Equation 5, the practical development length required for each bar stress level can be calculated. In Table 7, the experimental results for the development length are compared to the values proposed by the design codes. The values in Table 7 indicate that both design guidelines ACI440.1R-15 [46] and CSA-S806-12 [47] propose conservative development length values which are almost twice the tests ones. Moreover, there is a deficiency in calculating development length in fiber reinforced concrete in the both aforementioned design guidelines.

Fig. 17. Free diagram of tensile loaded bar embedded in concrete.

$$l_e \pi d_b u = A_f f_f \quad (4)$$

$$l_e = \frac{A_f f_f}{\pi d_b u} \quad (5)$$

3.7.1. ACI440.1R-15

ACI440.1R-15 [46] Design Code propose a development length and 90-degree bend in order to ensure the bonding strength between concrete and FRP bar. According to ACI440.1R-15 [46], Equation 6 is proposed to provide the required development length based on the experiments performed by Wambeke [48]. In this Equation, the parameters f_{fe}, f_{fu}, f'_c, α, l_e, d_b, and C are the stress developed at FRP rebar cross-section, FRP rebar failure stress, concrete compressive strength, rebar position correction coefficient, development length, bar diameter, and concrete cover, respectively. It should be noted that the proposed $\frac{C}{d_b}$ ratio should not exceed 3.5 in this Equation. The position correction coefficient, α, is also assumed 1, except for the cases where the rebar is horizontal and there is more than 300 mm concrete casting below it; so, in these cases the coefficient is considered 1.5. In the present study, α is assumed 1. It is worth mentioning that in Equation 6 there are not any parameters to address the effect of light-weight concrete and fiber reinforced concrete. The calculated values for the development length proposed by the code in accordance with the tensile stress level at the GFRP bar cross-section of each specimen are presented in Table 7. In order to have a better comprehension, the ratio of the development length proposed by the code to the experimental development length is also presented in Table 7 and Fig.18.

$$f_{fe} = \frac{0.083\sqrt{f'_c}}{\alpha}\left(13.6\frac{l_e}{d_b} + \frac{C}{d_b} \times \frac{l_e}{d_b} + 340\right) \le f_{fu} \quad (6)$$

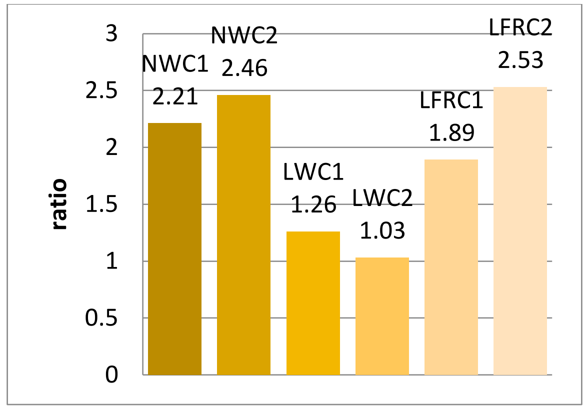

Fig. 18. The ratio of the development length proposed by ACI440.1R-15 [46] to the experimental development length.

3.7.2. CSA-S806-12

CSA-S806-12 [47] Design Code also proposes development length, using 90-degree hooks, and mechanical restraint in order to provide the required bond strength between the FRP bars and concrete. Therefore, Equation 7 is presented to calculate the development length. In this Equation, l_d, d_{cs}, f'_c, f_f, and A_b are development length, concrete cover, concrete compressive strength, FRP rebar end tension, and FRP rebar cross section, respectively. Also, the correction coefficients k_1, k_2, k_3, k_4, and k_5 are related to the rebar position, concrete specific gravity, rebar size, rebar fiber type, and rebar surface type, respectively. It should be noted that in the Equation proposed by CSA-S806-12 [47], the effect of concrete's specific gravity is taken into account by k_2; but the impact of fibers and their ability to reduce the development length is not considered. The calculated values for the development length proposed by the code in accordance with the tensile stress level at the GFRP bar cross-section of each specimen are presented in Table 7. In addition, the ratio of the development length proposed by CSA-S806-12 [47] to the experimental development length is also presented in Table 7 and Fig. 19.

$$l_d = 1.15 \frac{k_1 k_2 k_3 k_4 k_5}{d_{cs}} \times \frac{f_f}{\sqrt{f'_c}} A_b \qquad (7)$$

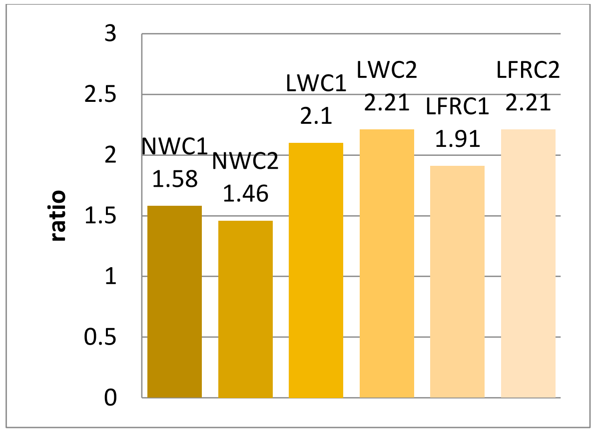

Fig. 19. The ratio of the development length proposed by CSA-S806-12 [47] to the experimental development length.

Table 7. Comprative results of the development length suggested by the design codes

Specimen code	Maximum tensile stress	Experimental development length	ACI440.1R-15 [46]		CSA-S806-12 [47]	
	f_f (MPa)	l_{exp} (mm)	l_e (mm)	$\frac{l_e}{l_{exp}}$	l_d (mm)	$\frac{l_d}{l_{exp}}$
NWC1	309.51	80	177	2.21	126	1.58
NWC2	388.93	80	197	2.46	117	1.46
LWC1	235.27	80	101	1.26	168	2.1
LWC2	259.76	80	82	1.03	177	2.21
LFRC1	339.17	80	151	1.89	153	1.91
LFRC2	383.96	80	202	2.53	177	2.21

4. Conclusion

The results of the direct pull-out test on 18 specimens which are made of different types of concrete such as normal-weight, light-weight, and light-weight fiber reinforced concrete come to the following conclusion:

1- Without using a proper mechanical restrained system for GFRP bar, the bond strength between bar and concrete is lost which may cause pre-mature failure in the concrete members.
2- Increasing compressive strength in both normal-weight and light-weight concrete leads to the enhancement of the bond strength.
3- The increase of compressive strength in normal-weight concrete causes relatively higher bond strength in comparison with light-weight concrete.
4- The inherent weakness of light-weight aggregate inter-locking could be eliminated using macro-fibers.
5- GFRP bars are inherently weak, having the bond strength with concrete due to their shape and inadequate mechanical friction. This deficiency should be considered in the design approach by using a proper restraint system.
6- Existing design codes such as ACI440.1R-15 and CSA-S806-12 provide conservative development lengths for GFRP bar. This matter is

explainable regarding the fact that GFRP bar bond strength is highly depends on many factors such as physical shape, diameter, ribs configuration, and so on.

7- There is lack of information about the effect of using different types of concrete such as fiber reinforced concrete on the bond strength in the existing design codes.

REFERENCES

[1] Hao, Q. D., Wang, B., & Ou JP. Fiber reinforced polymer rebar's application to civil engineeringle. Concrete 2006;9:38–40.

[2] Bazli M, Ashrafi H, Oskouei AV. Effect of harsh environments on mechanical properties of GFRP pultruded profiles. Composites Part B: Engineering 2016;99:203–15. doi:10.1016/j.compositesb.2016.06.019.

[3] J. Alves, A. El-Ragaby EE-S. Durability of GFRP bars' bond to concrete under different loading and environmental conditionstle. Compos Constr 2010;15:249–262.

[4] Feng P, Wang J, Wang Y, Loughery D, Niu D. Effects of corrosive environments on properties of pultruded GFRP plates. Composites Part B: Engineering 2014;67:427–33. doi:10.1016/j.compositesb.2014.08.021.

[5] Hamedmirjafari B, Bolouri Bazzaz J, Abrishami S. Calibration of bar-Concrete Bond Stress Relationships for Bond Stress Prediction of GFRP Soil Nails Using Experimental Pullout Tests. Journal of Rehabilitation in Civil Engineering 2019;0:18–36. doi:10.22075/jrce.2019.14856.1279.

[6] Saleh N, Ashour A, Lam D, Sheehan T. Experimental investigation of bond behaviour of two common GFRP bar types in high – Strength concrete. Construction and Building Materials 2019;201:610–22. doi:10.1016/j.conbuildmat.2018.12.175.

[7] Hosseini G. Capacity Prediction of RC Beams Strengthened with FRP by Artificial Neural Networks Based on Genetic Algorithm. Soft Computing in Civil Engineering 2017;1:93–8. doi:10.22115/scce.2017.48392.

[8] Naderpour H, Nagai K, Fakharian P, Haji M. Innovative models for prediction of compressive strength of FRP-confined circular reinforced concrete columns using soft computing methods. Composite Structures 2019;215:69–84. doi:10.1016/j.compstruct.2019.02.048.

[9] Soong WH, Raghavan J, Rizkalla SH. Fundamental mechanisms of bonding of glass fiber reinforced polymer reinforcement to concrete. Construction and Building Materials 2011;25:2813–21. doi:10.1016/j.conbuildmat.2010.12.054.

[10] Golafshani EM, Rahai A, Sebt MH. Bond behavior of steel and GFRP bars in self-compacting concrete. CONSTRUCTION & BUILDING MATERIALS 2014;61:230–40. doi:10.1016/j.conbuildmat.2014.02.021.

[11] Benmokrane B, Maceachern M, That TT ZB. Evaluation of bond characteristics of GFRP rebars embedded in polymer and normal cement concrete. 1999.

[12] Al-Zahrani MM. Bond behavior of fiber reinforced plastic reinforcements with concrete. Pennsylvania State University, 1995.

[13] Soares S, Freitas N, Pereira E, Nepomuceno E, Pereira E, Sena-Cruz J. Assessment of GFRP bond behaviour for the design of sustainable reinforced seawater concrete structures. Construction and Building Materials 2020;231. doi:10.1016/j.conbuildmat.2019.117277.

[14] Zemour N, Asadian A, Ahmed EA, Khayat KH, Benmokrane B. Experimental study on the bond behavior of GFRP bars in normal and self-consolidating concrete. Construction and Building Materials 2018;189:869–81. doi:10.1016/j.conbuildmat.2018.09.045.

[15] Di B, Wang J, Li H, Zheng J, Zheng Y, Song G. Investigation of bonding

behavior of FRP and steel bars in self-compacting concrete structures using acoustic emission method. Sensors (Switzerland) 2019;19:1–14. doi:10.3390/s19010159.

[16] Mazaheripour H, Barros JAO, Sena-Cruz JM, Pepe M, Martinelli E. Experimental study on bond performance of GFRP bars in self-compacting steel fiber reinforced concrete. Composite Structures 2013;95:202–12. doi:10.1016/j.compstruct.2012.07.009.

[17] Almeida Filho FM, El Debs MK, El Debs ALHC. Numerical approach of the bond stress behavior of steel bars embedded in self-compacting concrete and in ordinary concrete using beam models. Revista IBRACON de Estruturas e Materiais 2013;6:499–512. doi:10.1590/s1983-41952013000300009.

[18] Al-Zahrani MM, Al-Dulaijan SU, Nanni A, Bakis CE, Boothby TE. Evaluation of bond using FRP rods with axisymmetric deformations. Construction and Building Materials 1999;13:299–309. doi:10.1016/S0950-0618(99)00038-0.

[19] Huang H, Yuan Y, Zhang W, Hao R, Zeng J. Bond properties between GFRP bars and hybrid fiber-reinforced concrete containing three types of artificial fibers. Construction and Building Materials 2020;250:118857. doi:10.1016/j.conbuildmat.2020.118857.

[20] Patil SB, Manjunatha GS. Experimental study on bond strength of GFRP bars. Materials Today: Proceedings 2020;21:1044–9. doi:10.1016/j.matpr.2020.01.003.

[21] Okelo R, Yuan RL. Bond Strength of Fiber Reinforced Polymer Rebars in Normal Strength Concrete. Journal of Composites for Construction 2005;9:203–13. doi:10.1061/(ASCE)1090-0268(2005)9:3(203).

[22] Ashrafi H, Bazli M, Oskouei AV. Enhancement of bond characteristics of ribbed-surface GFRP bars with concrete by using carbon fiber mat anchorage. Construction and Building Materials 2017;134:507–19. doi:10.1016/j.conbuildmat.2016.12.083.

[23] Doostmohamadi A, Karamloo M, Afzali-Naniz O. Effect of polyolefin macro fibers and handmade GFRP anchorage system on improving the bonding behavior of GFRP bars embedded in self-compacting lightweight concrete. Construction and Building Materials 2020;253:119230. doi:10.1016/j.conbuildmat.2020.119230.

[24] Ghoddousi P, Abbasi AM, Shahrokhinasab E, Abedin M. Prediction of Plastic Shrinkage Cracking of Self-Compacting Concrete. Advances in Civil Engineering 2019;2019.

[25] Mazloom M, Soltani A, Karamloo M, Hassanloo A, Ranjbar A. Effects of silica fume, superplasticizer dosage and type of superplasticizer on the properties of normal and selfcompacting concrete. Advances in Materials Research (South Korea) 2018;7:407–34. doi:10.12989/amr.2018.7.1.407.

[26] Karamloo M, Mazloom M, Payganeh G. Influences of water to cement ratio on brittleness and fracture parameters of self-compacting lightweight concrete. Engineering Fracture Mechanics 2016;168:227–41. doi:10.1016/j.engfracmech.2016.09.011.

[27] Varona FB, Baeza FJ, Bru D, Ivorra S. Evolution of the bond strength between reinforcing steel and fibre reinforced concrete after high temperature exposure. Construction and Building Materials 2018;176:359–70. doi:10.1016/j.conbuildmat.2018.05.065.

[28] Garber D, Shahrokhinasab E. Performance Comparison of In-Service, Full-Depth Precast Concrete Deck Panels to Cast-in-Place Decks. Accelerated Bridge Construction University Transportation Center (ABC-UTC); 2019.

[29] Fakharifar M, Dalvand A, Arezoumandi M, Sharbatdar MK, Chen G, Kheyroddin A. Mechanical properties of high performance fiber reinforced cementitious composites. Computers and Chemical Engineering 2014;71:510–20. doi:10.1016/j.conbuildmat.2014.08.068.

[30] Karamloo M, Afzali-Naniz O,

Doostmohamadi A. Impact of using different amounts of polyolefin macro fibers on fracture behavior, size effect, and mechanical properties of self-compacting lightweight concrete. Construction and Building Materials 2020;250:118856. doi:10.1016/j.conbuildmat.2020.118856.

[31] Veljkovic A, Carvelli V, Haffke MM, Pahn M. Concrete cover effect on the bond of GFRP bar and concrete under static loading. Composites Part B: Engineering 2017;124:40–53. doi:10.1016/j.compositesb.2017.05.054.

[32] D7913M-14 AD/. Standard Test Method for Bond Strength of Fiber-Reinforced Polymer Matrix Composite Bars to Concrete by Pullout Testing. ASTM International: American Standard Test Method; 2014.

[33] Bazli M, Ashrafi H, Oskouei AV. Experiments and probabilistic models of bond strength between GFRP bar and different types of concrete under aggressive environments. Construction and Building Materials 2017;148:429–43. doi:10.1016/j.conbuildmat.2017.05.046.

[34] Kotynia R, Szczech D, Kaszubska M. Bond Behavior of GRFP Bars to Concrete in Beam Test. Procedia Engineering 2017;193:401–8. doi:10.1016/j.proeng.2017.06.230.

[35] Moreno C, Bastos AM. Experimental and Numerical Evaluation of Bond Properties Between Reinforcement and Concrete. 5th International Conference on Mechanics and Materials in Design 2006:1–17.

[36] Antonietta Aiello M, Leone M, Pecce M. Bond Performances of FRP Rebars-Reinforced Concrete. Journal of Materials in Civil Engineering 2007;19:205–13. doi:10.1061/(ASCE)0899-1561(2007)19:3(205).

[37] De Almeida Filho FM, El Debs MK, El Debs ALHC. Bond-slip behavior of self-compacting concrete and vibrated concrete using pull-out and beam tests. Materials and Structures/Materiaux et Constructions 2008;41:1073–89. doi:10.1617/s11527-007-9307-0.

[38] Gooranorimi O, Claure G, Suaris W, Nanni A. Bond-slip effect in flexural behavior of GFRP RC slabs. Composite Structures 2018;193:80–6. doi:10.1016/j.compstruct.2018.03.027.

[39] Gooranorimi O, Suaris W, Nanni A. A model for the bond-slip of a GFRP bar in concrete. Engineering Structures 2017;146:34–42. doi:10.1016/j.engstruct.2017.05.034.

[40] ASTM C1116. Standard Specification for Fiber-Reinforced Concrete. 2010.

[41] ASTM D7205 / D7205M-06(2016). Standard Test Method for Tensile Properties of Fiber Reinforced Polymer Matrix Composite Bars. West Conshohocken PA; 2016. doi:10.1520/D7205_D7205M-06R16.

[42] ASTM D7508. Standard Specification for Polyolefin Chopped Strands for Use in Concrete. 2010.

[43] ASTM D2256. Standard Test Method for Tensile Properties of Yarns by the Single-Strand Method. 2010.

[44] Canadian Standards Association. Design and Construction of Building Components with Fibrereinforced Polymers. 2002.

[45] Navas FO, Navarro-gregori J, Herdocia GL, Serna P, Cuenca E. An experimental study on the shear behaviour of reinforced concrete beams with macro-synthetic fibres. Construction and Building Materials 2018;169:888–99. doi:10.1016/j.conbuildmat.2018.02.023.

[46] ACI Committee 440.1R. Guide for the Design and Construction of Structural Concrete Reinforced with Fiber-Reinforced Polymer Bars. 2015.

[47] Canadian Standards Association. S806-12. Design And Construction Of Building Structures With Fibre-Reinforced Polymers 2012.

[48] Wambeke, B. W., & Shield CK. Development length of glass fiber-reinforced polymer bars in concrete. ACI Structural Journal 2006;103:11.